The Expansion of the Forward Shock of 1E 0102.2-7219 in X-rays

Paul Plucinsky(CfA), Long Xi (IHEP,CAS), Terrance Gaetz(CfA), John Hughes (Rutgers) & Daniel Patnaude (CfA)

Xi et al. 2019, ApJ, 874, 14

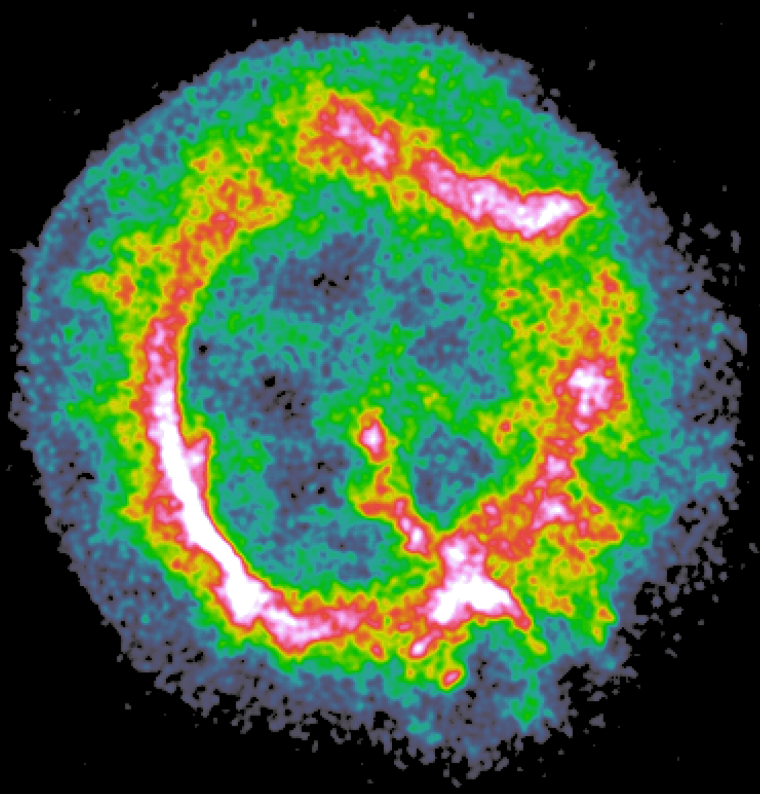

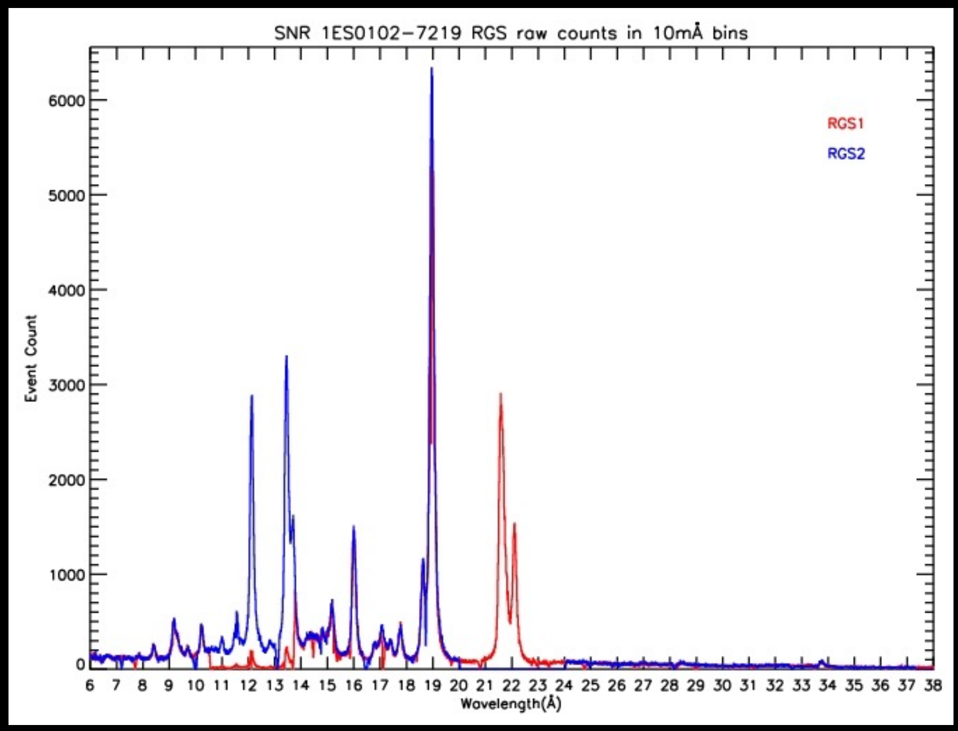

1E 0102.2 -7219: Introduction

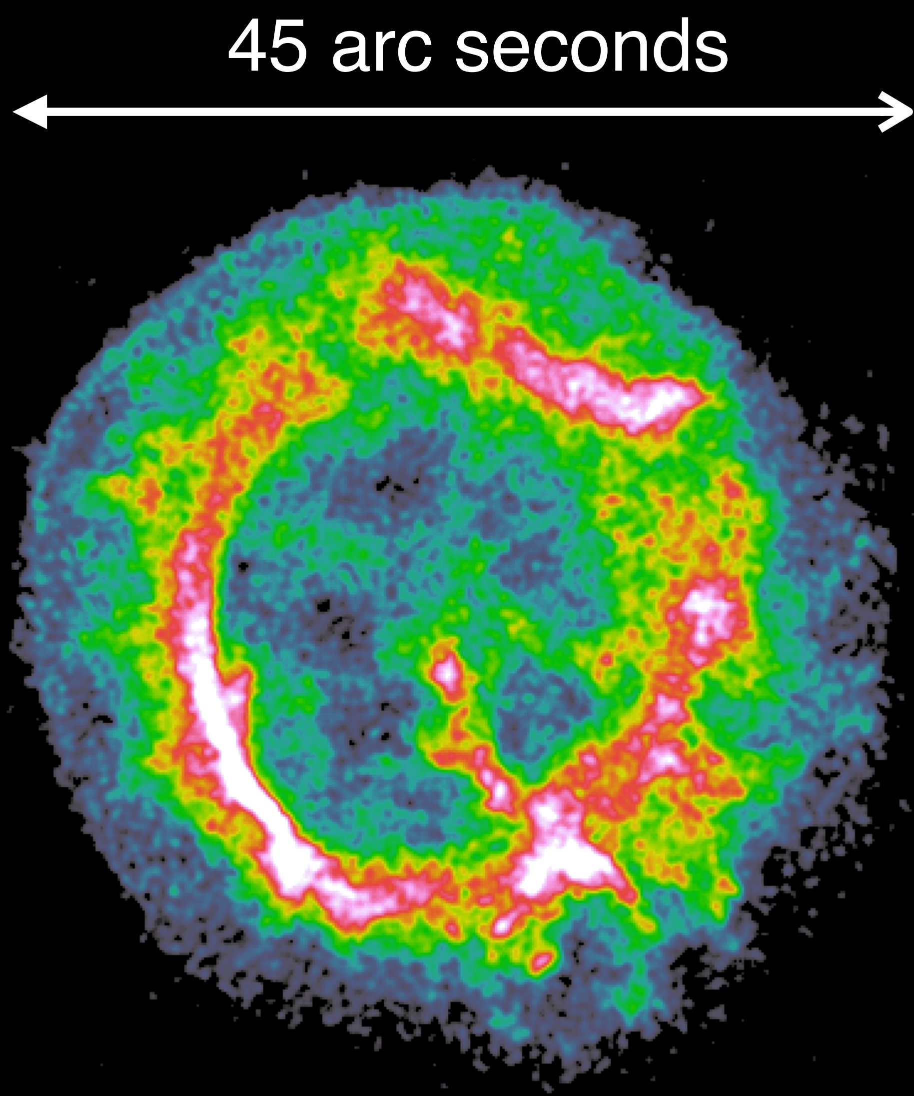

- hereafter called "E0102"
- X-ray brightest SNR in the SMC
- ~0.75 arcmin diameter, ~13 pc
- t ~ 2,050 yr (Finkelstein et al. 2006)
- L_X(0.3-10.0 kev) = 1.1×10^{37} ergs s^{-1}
- "O-rich" SNR, core-collapse SNe (Dopita et al. 1981)
- O, Ne, Mg, & Si abundances most consistent with a ~25 $M_\odot$ progenitor (Blair et al. 2000)
- compact object, L=1.4×10^{33} ergs s^{-1} [1.2-2.0 keV] (Vogt et al. 2018)
- X-ray morphology is roughly symmetric

ACIS S3 (0.35-8.0 keV), OBSID 1423, 19 ks, 10/1999

E0102's Simple X-ray Morphology

E0102 has a simple morphology which we will take advantage of in this analysis.
Kuranz et al. 2018

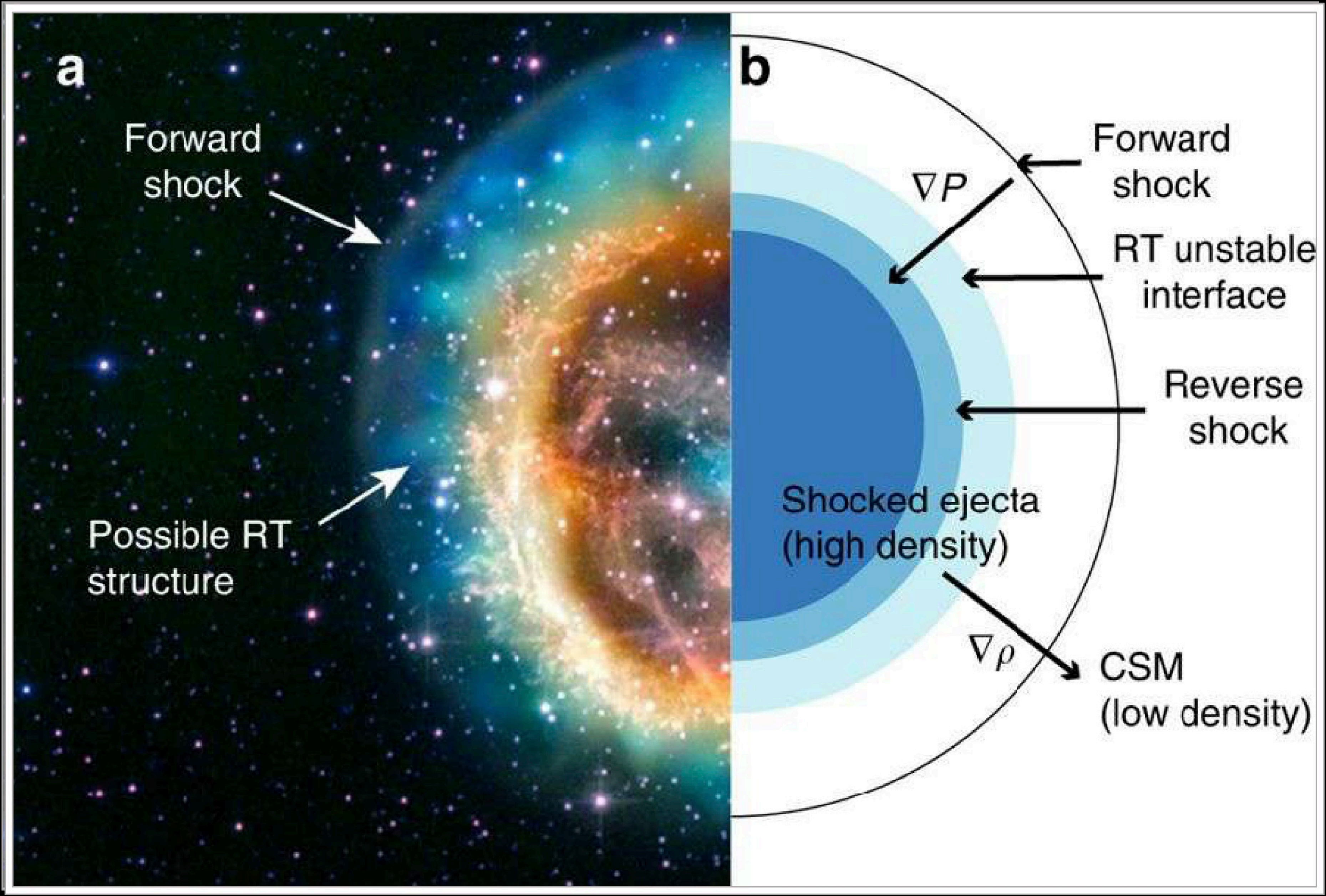

X-ray vs. Optical Morphology

Finkelstein et al. 2006

X-ray and optical are sometime correlated, sometimes anti-correlated, in general the optical is more complicated

HST ACS [O III] Chandra ACIS S3

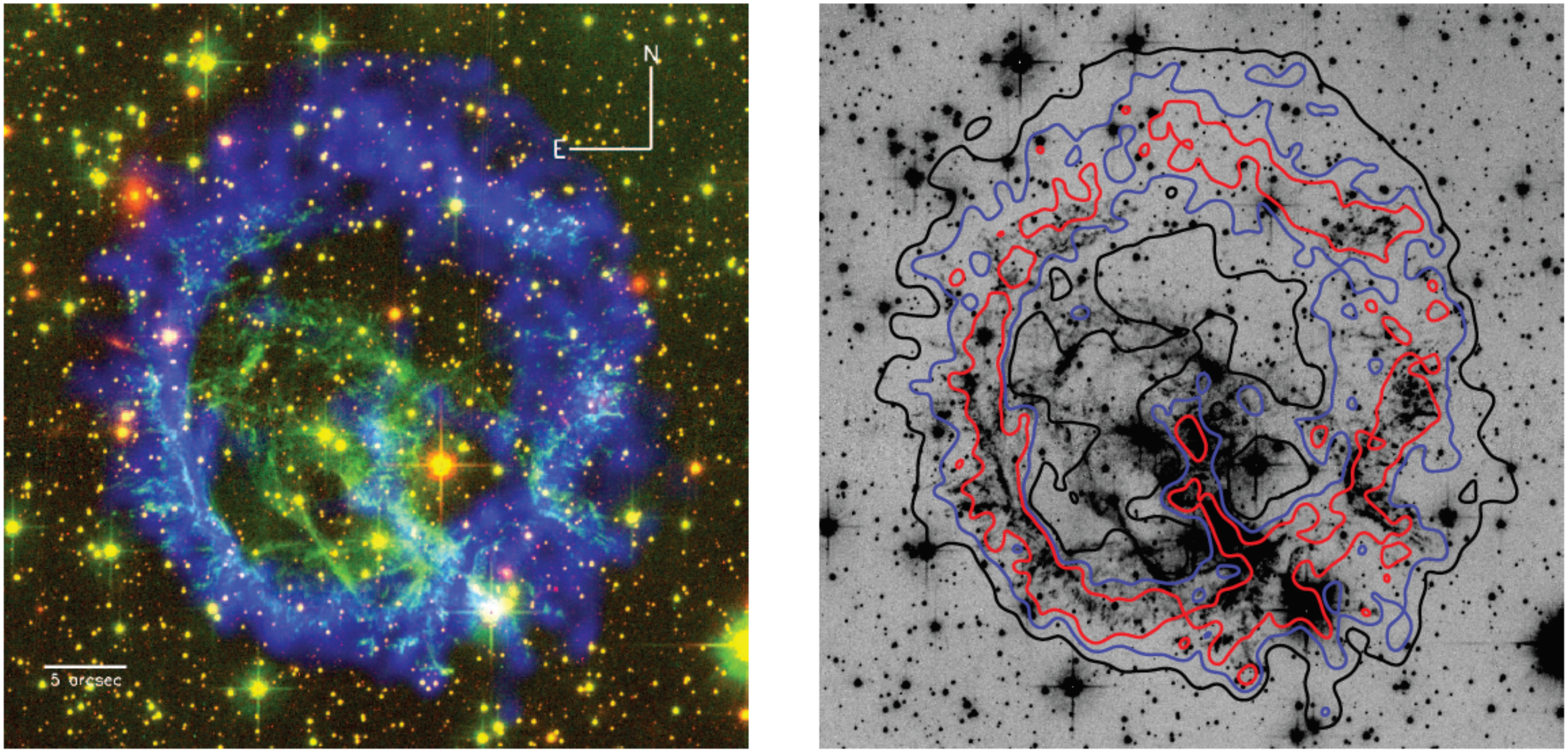

FIG. 7.—*Left*: Three-color image, with the ACS 2003 [O III] in green and the F775W filter in red. The 1999 *Chandra* image is represented in blue. *Right*: ACS 2003 epoch shown with contours from the 1999 *Chandra* image overlaid. The red contour marks the brightest X-ray emission and is coincident with the reverse shock, while the black contour outlines the faintest emission with the outer edge at the position of the forward blast wave. The X-ray and optical ejecta emissions correspond in many areas, but are also anticorrelated in several regions.

1E 0102.2 -7219: X-ray Spectrum

XMM-Newton RGS spectrum Pollock (Sheffield), Rasmussen et al. 2000
Spectrum is dominated by strong lines of O, Ne and Mg with *little or no Fe emission*
This is the simplest known SNR spectrum in the 0.5 - 1.0 keV band

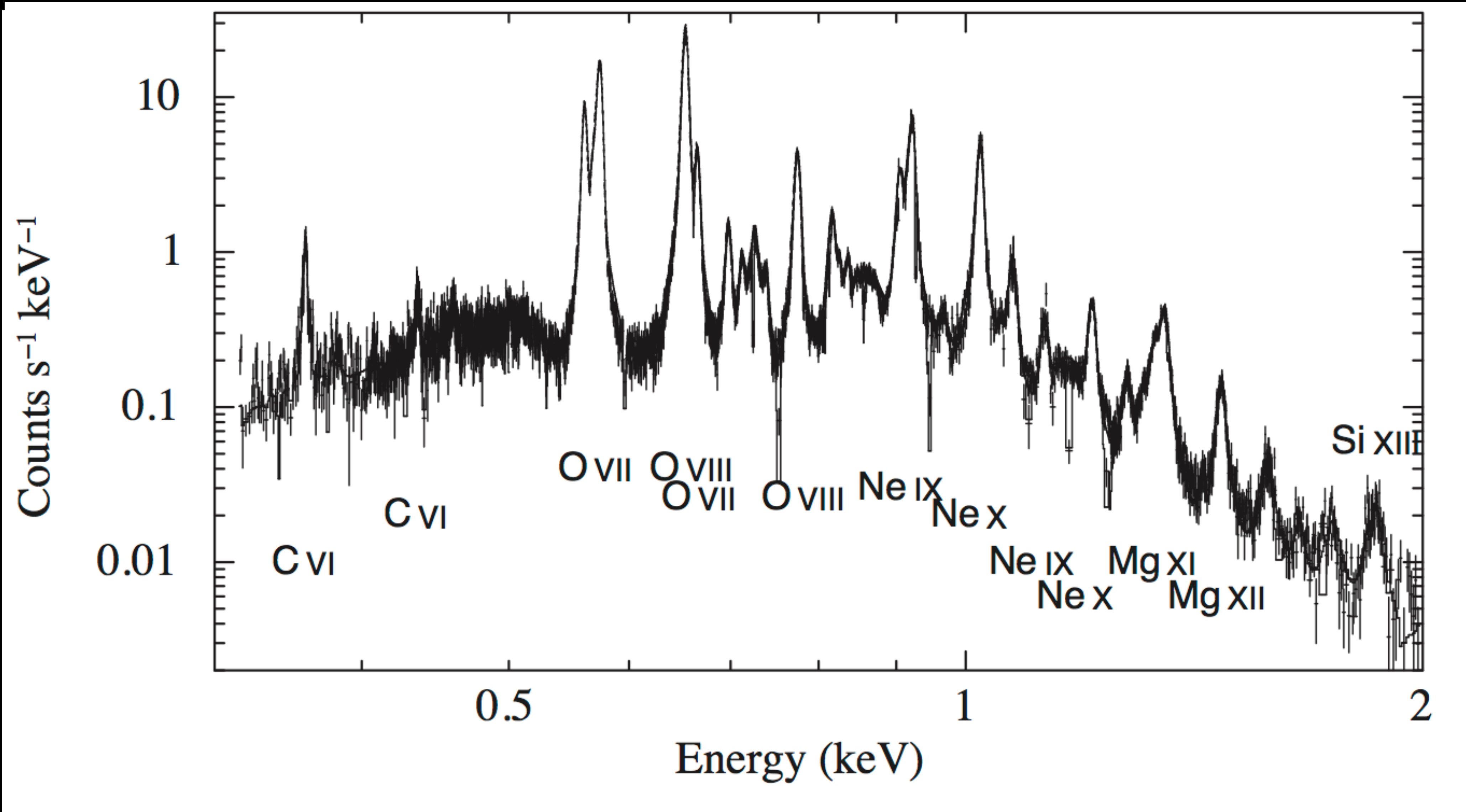

The Expansion of E0102 in X-rays

- Hughes et al. 2000 compared an early (1999) Chandra image to ROSAT/HRI to Einstein/HRI images and derived an expansion of 0.100 %/yr +/- 0.025 %/yr or 0.022 arcsec/yr which implies a shock velocity of v_S~6,000 km/s
- X-ray spectral fits give kT=0.4 - 1.0 keV for the shock, while a v_S~6,000 km/s naively indicates a temperature kT~45 keV
- Nonequipartition between electrons and ions can explain part of this discrepancy but they can't get the electron temperature below 2.5 keV even assuming no equipartition
- Hughes et al. 2000 conclude that a significant fraction of the shock's energy must be going into the acceleration of cosmic rays (CRs)
- Their fitting method estimates the "global mean expansion" and assumes that the expansion rate is uniform over the entire remnants both radially and azimuthally.
- They estimate an age of ~1000 yr.

Hughes et al. 2000

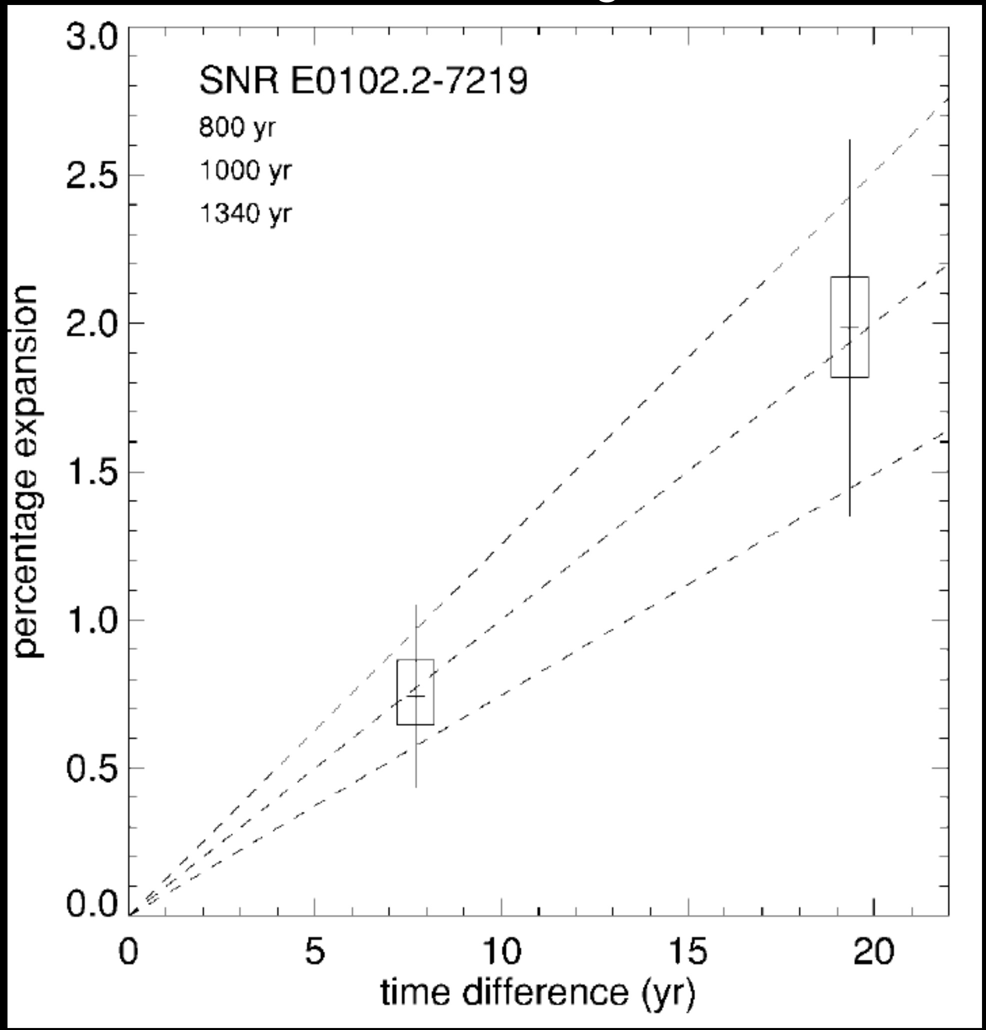

The Expansion of E0102 in X-rays

- Hughes et al. 2000 compared an early (1999) Chandra image to ROSAT/HRI to Einstein/HRI images

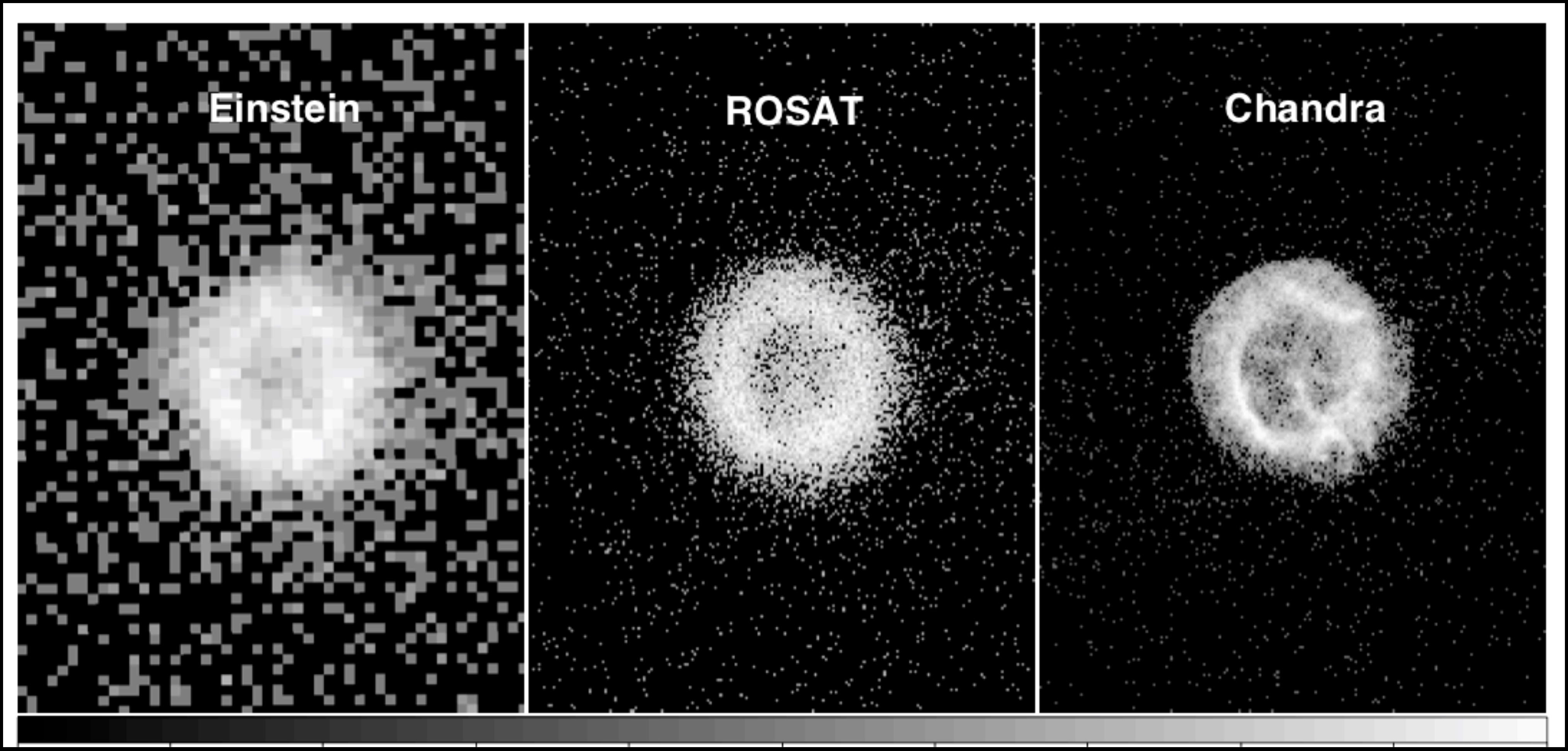

A Different and Hopefully Simpler Approach

1. Use only Chandra data and compare Chandra data to Chandra data. Remove systematic uncertainties in ROSAT and Einstein data.

2. Measure the expansion of the *outer blast wave*, exclude the bright ring. Exploit Chandra's angular resolution to separate the blast wave from the ejecta ring.

3. Minimize or eliminate pileup by looking at the outer blast wave and/or using subarray data with a shorter frametime.

Complications with Our Approach

1. The mirror is certainly the same for each measurement but ACIS is a different detector every time it observes E0102 due to the time-variable contamination layer.

2. The outer blast wave is faint and the statistics can be poor for an 8 ks observation.

3. Subarray data may have no point sources to register on. We must find another way to register the images. All data since 2006 are in subarray mode.

Long XI (IHEP,CAS) does all the hard work

Registration of the X-ray Data

Register on the bright central knot, since subarray data of 10-20 ks may not have any sources that are bright enough to register on.

There are 11 ACIS S3 on-axis subarray observations from 2003 to 2016.

HST WFPC3/UVIS data, courtesy of D. Milisavljevic (Purdue)
[O III]
Blue == blue-shifted (v< -1500 km s^{-1})
Red == red-shifted (v> 1500 km s^{-1})
Green == ~zero velocity
(-2000 < v < 2000 km s^{-1})

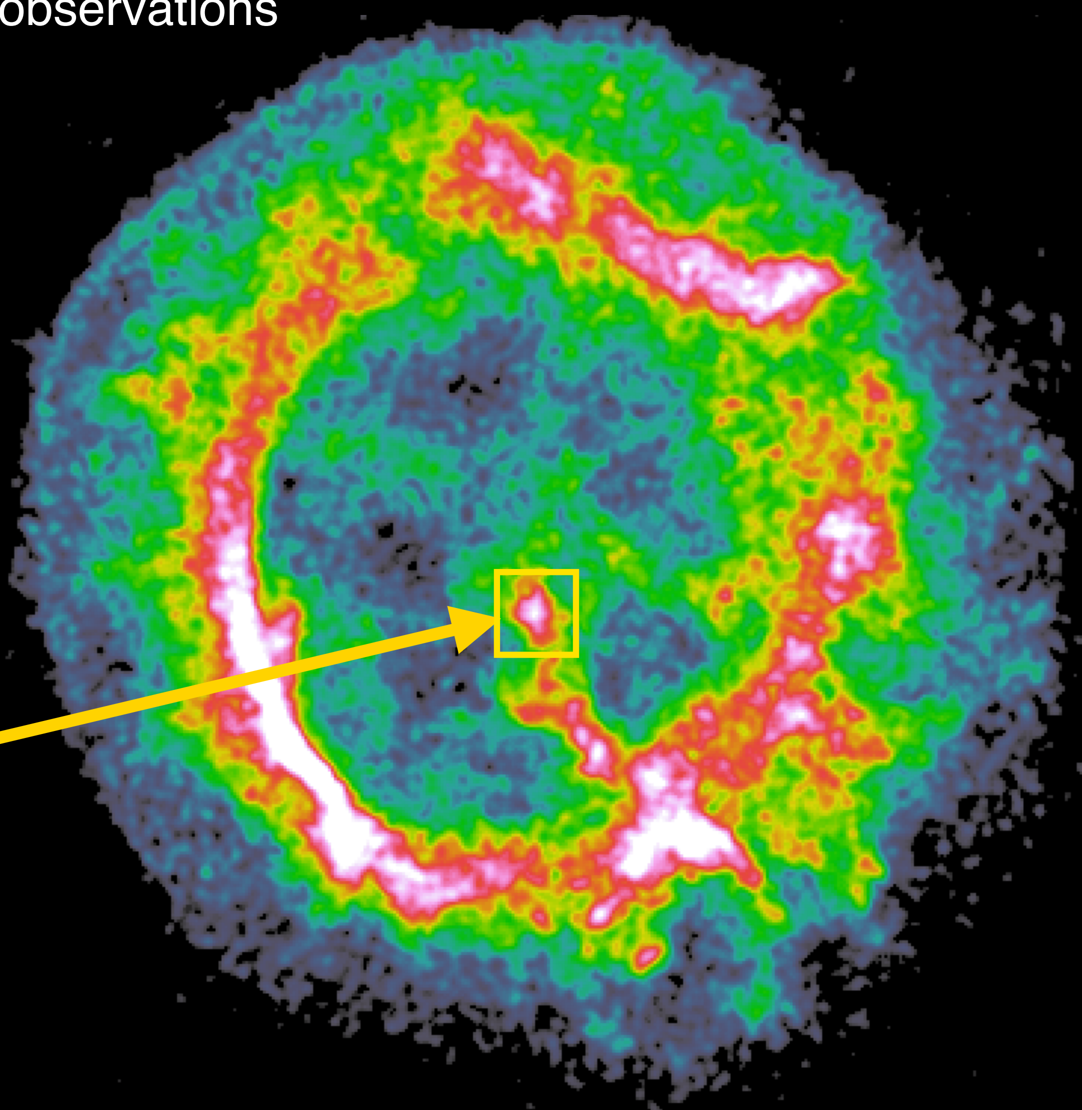

Central Knot to register on

Definition of Annular Regions

Xi et al. 2019 ApJ, 874, 14

A model is constructed based on early mission data. Later subarray observations are registered relative to that image. Radial profiles are extracted and fit in the following regions.

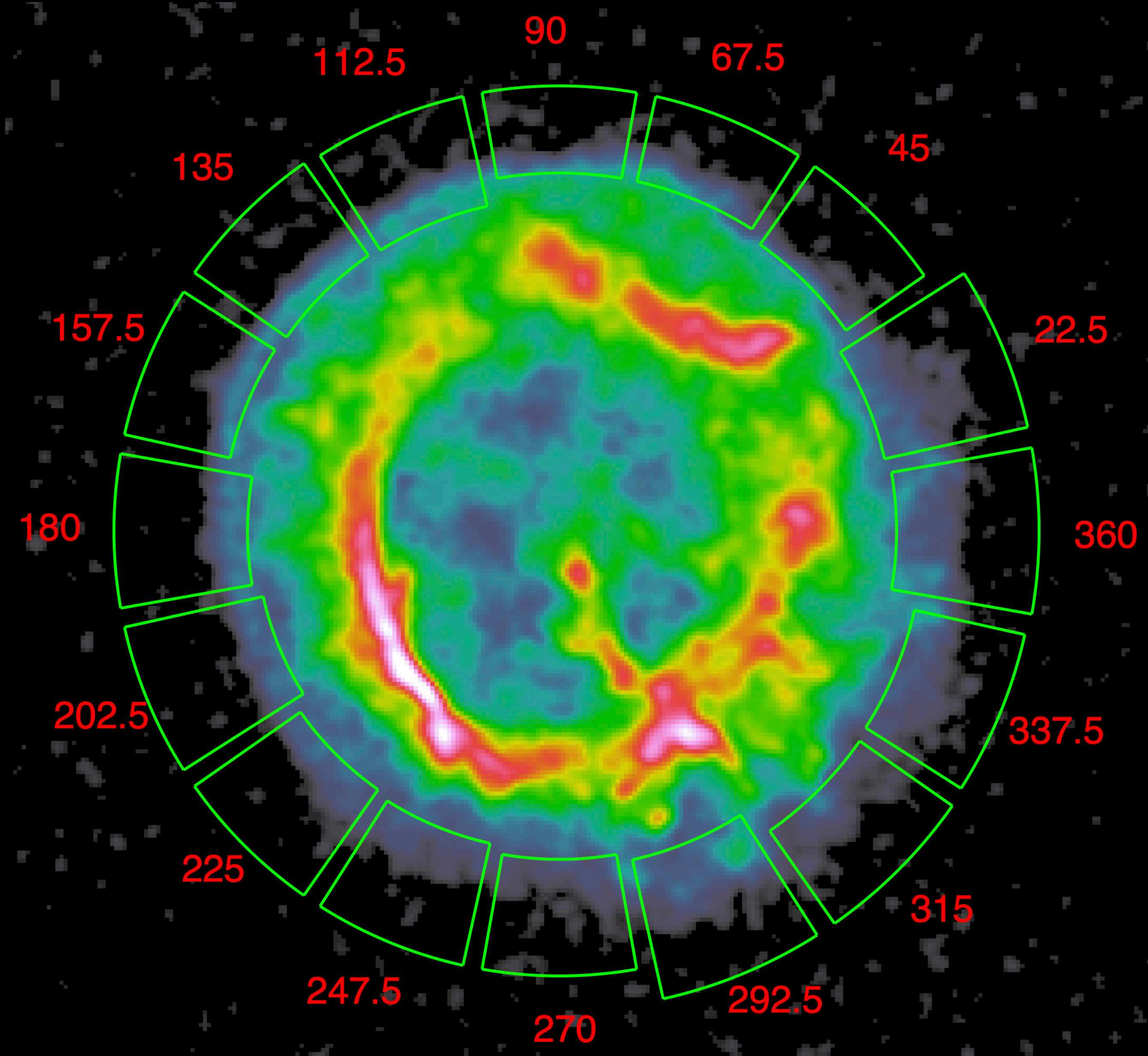

Expansion Rate Results

Xi et al. 2019

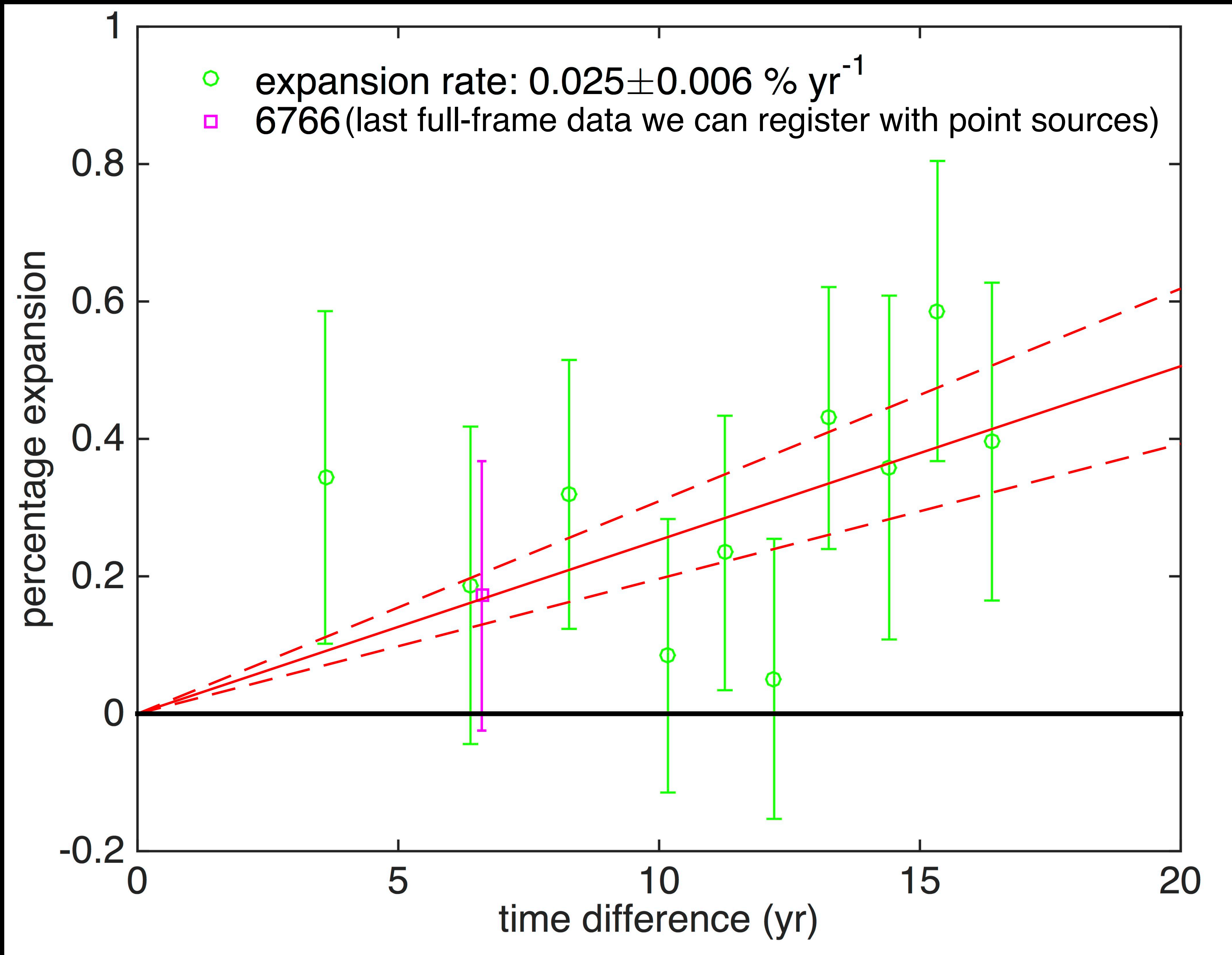

Forward and Reverse Shock Radii

Xi et al. 2019

We can take advantage of E0102's simple geometry and *Chandra*'s superb resolution to measure the position of the forward and reverse shocks. Ellipses were fit to determine the forward and reverse shock radii.

Fitted Values:

v_b = 1614+/- 367 km s^{-1}

R_b = 6.34 +/- 0.10 pc

R_r = 4.17 +/- 0.12 pc

X Milisavljevic center

O Finkelstein center

+ reverse shock center

◇ forward shock center

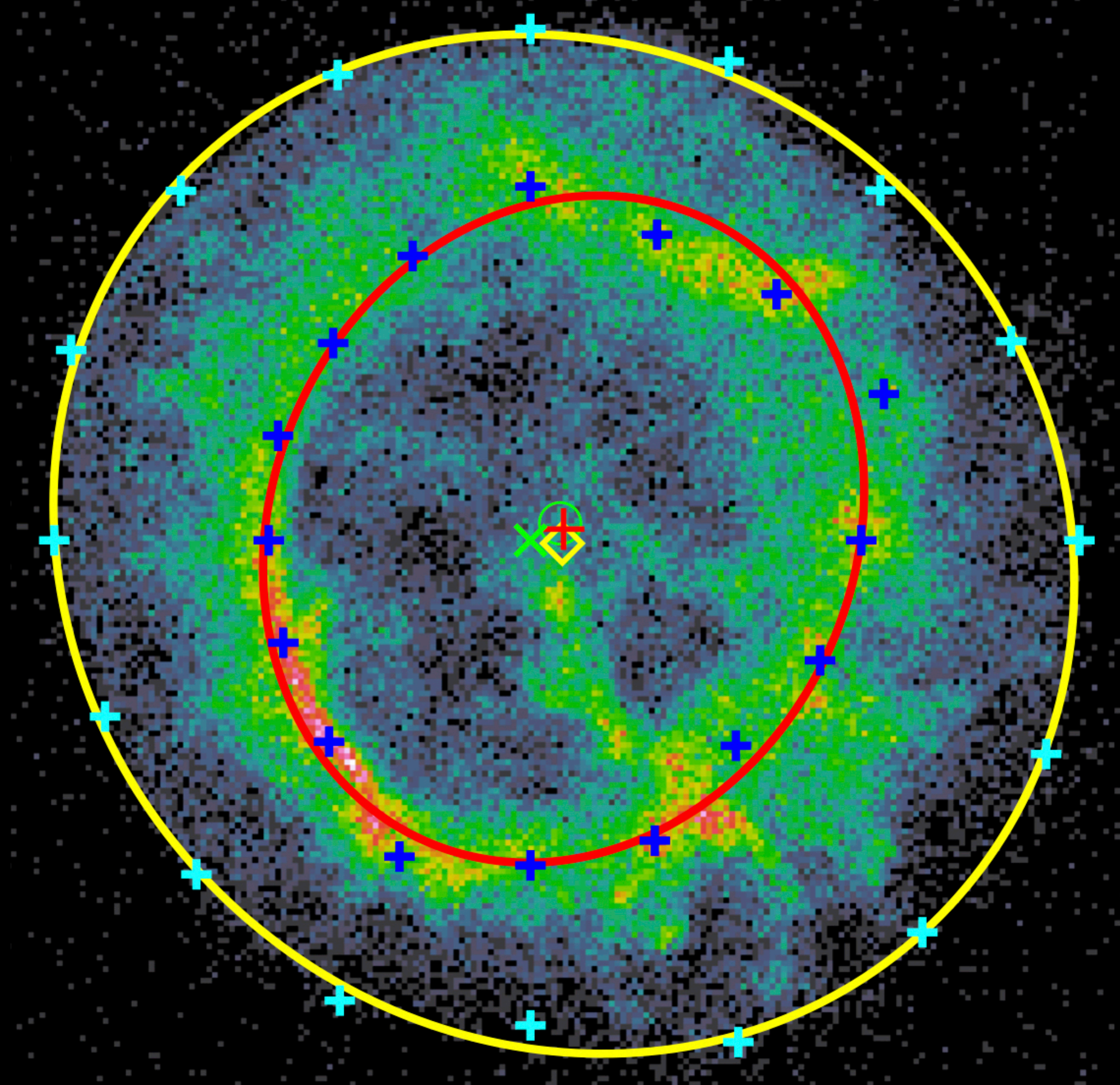

Spectral Fits

Xi et al. 2019

- Spectral fits indicate the blast wave region has abundances typical of the SMC
- Spectral fits indicate the "near finger" and "central knot" have significantly enhanced abundances

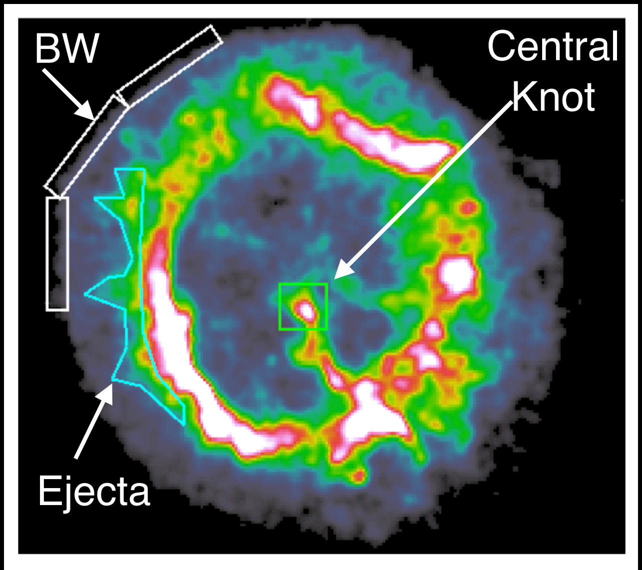

Parameters	Blast wave	Ejecta	Center bright feature
kT(keV)	0.76 ± 0.05	0.63 ± 0.02	1.17 ± 0.08
$n_e t(10^{11} cm^{-3} s)$	1.81 ± 0.32	9.05 ± 1.18	1.66 ± 0.32
$N_{H,SMC}(10^{20} cm^{-3})$	4.85 ± 1.81	6.81 ± 1.18	6.17 ± 0.88
Oxygen	0.29 ± 0.05	2.13 ± 0.28	2.46 ± 0.21
Neon	0.36 ± 0.04	3.02 ± 0.41	4.56 ± 0.36
Magnesium	0.27 ± 0.05	1.30 ± 0.18	2.23 ± 0.21
Iron	0.13 ± 0.02	0.1 ± 0.02	0.19 ± 0.06
$C-statistic$(dof)	553.25(488)	503.13(488)	664.17(488)

Blast Wave

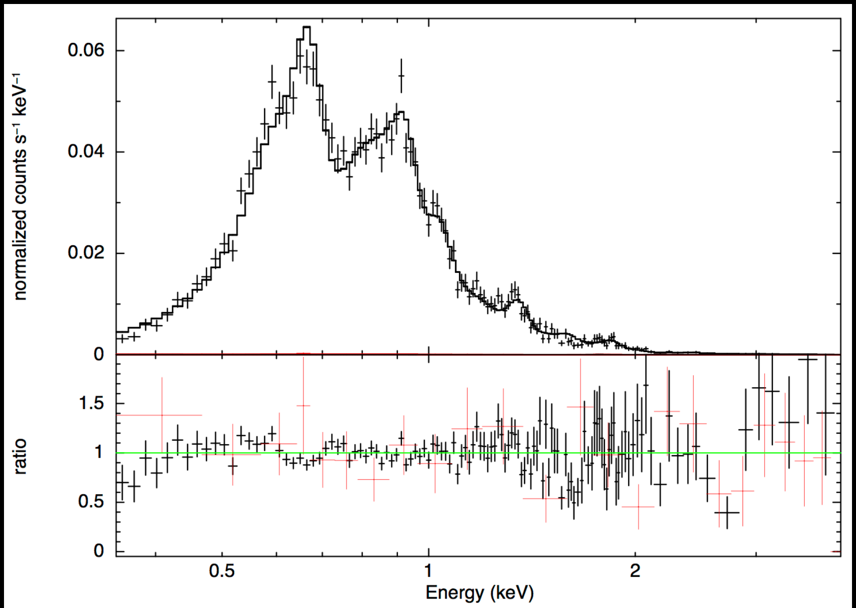

Ejecta

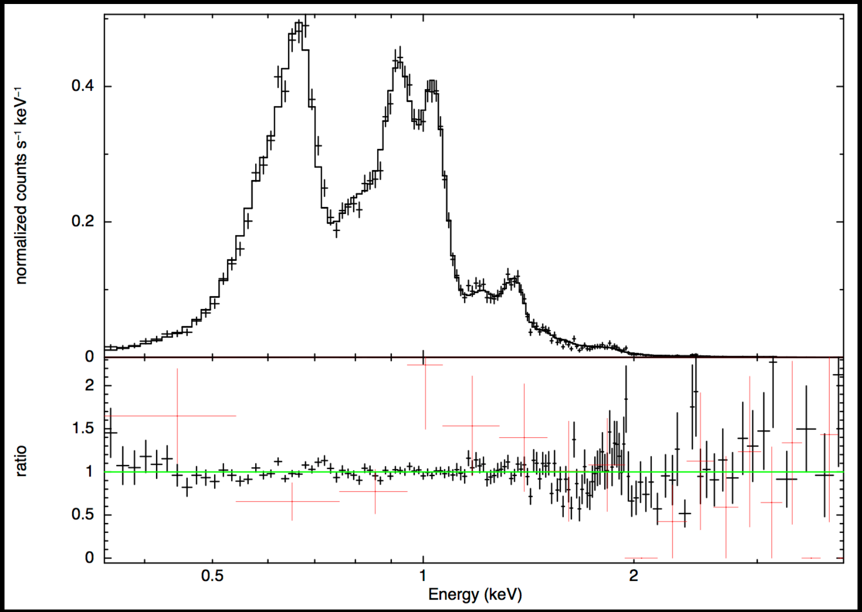

Blastwave Spectral Fits

Xi et al 2019

- Fit the blast wave region with a single component model (vpshock) and achieve acceptable fits
- abudances are consistent with SMC ISM abundances
- Compute an emission-weighted average temperature

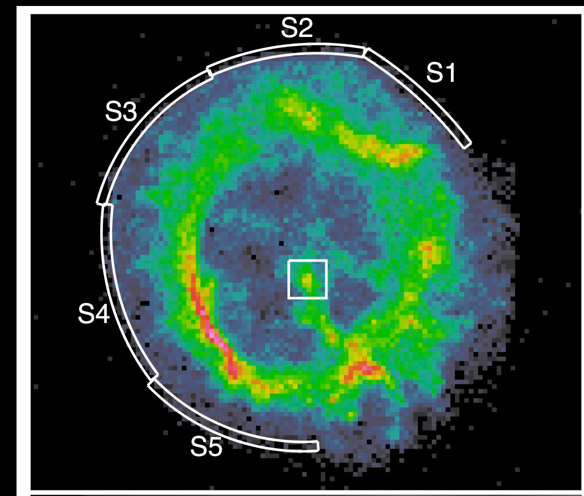

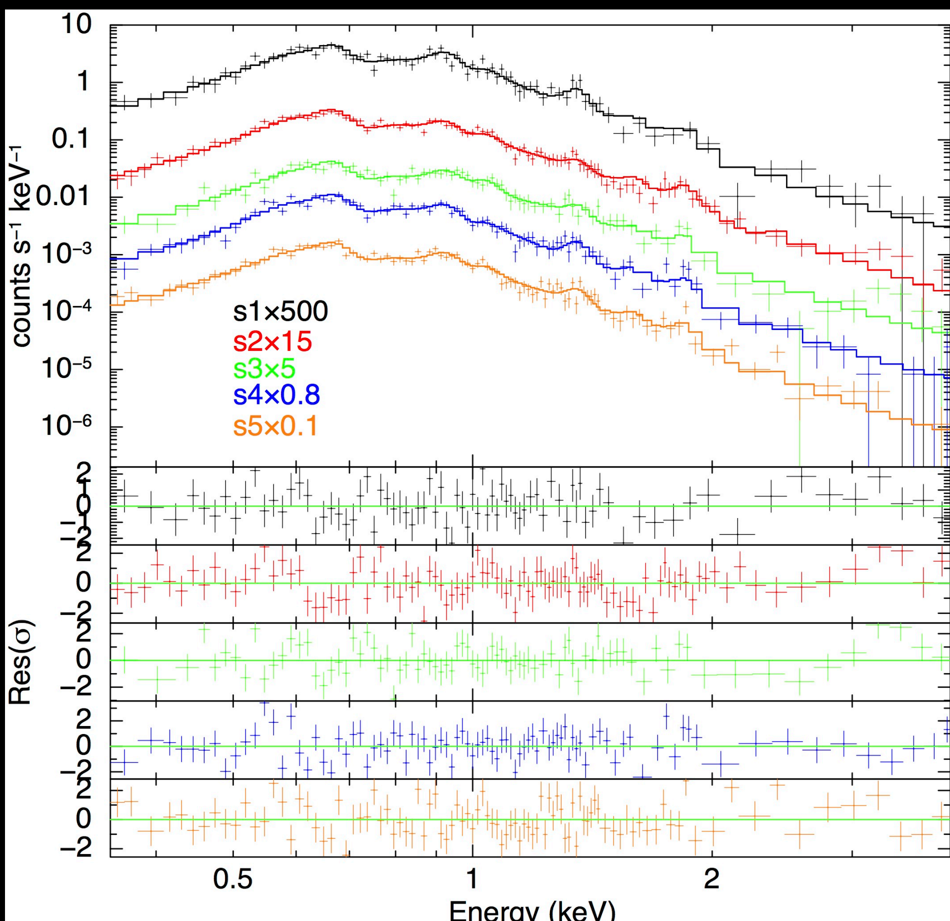

Parameters	S1	S2	S3	S4	S5
$kT_e\,(keV)$	$0.65^{+0.14}_{-0.07}$	$0.75^{+0.06}_{-0.05}$	$0.70^{+0.09}_{-0.11}$	$0.71^{+0.10}_{-0.08}$	$0.61^{+0.06}_{-0.04}$
Oxygen	$0.23^{+0.05}_{-0.04}$	$0.27^{+0.05}_{-0.04}$	$0.29^{+0.10}_{-0.06}$	$0.27^{+0.04}_{-0.04}$	$0.24^{+0.05}_{-0.04}$
Neon	$0.37^{+0.07}_{-0.05}$	$0.29^{+0.04}_{-0.03}$	$0.36^{+0.07}_{-0.06}$	$0.36^{+0.06}_{-0.05}$	$0.31^{+0.04}_{-0.04}$
Magnesium	$0.30^{+0.10}_{-0.08}$	$0.13^{+0.04}_{-0.04}$	$0.20^{+0.09}_{-0.07}$	$0.30^{+0.09}_{-0.08}$	$0.21^{+0.06}_{-0.05}$
Iron	$0.06^{+0.04}_{-0.02}$	$0.06^{+0.02}_{-0.01}$	$0.04^{+0.02}_{-0.02}$	$0.10^{+0.03}_{-0.03}$	$0.04^{+0.01}_{-0.01}$
$n_e t, (10^{11}\,\mathrm{cm^{-3}\,s})$	$1.50^{+0.99}_{-0.78}$	$1.53^{+0.51}_{-0.39}$	$2.32^{+2.83}_{-0.84}$	$1.10^{+0.59}_{-0.37}$	$2.24^{+0.93}_{-0.71}$
$Norm, (10^{-5})$	$2.02^{+0.51}_{-0.60}$	$4.76^{+0.57}_{-0.58}$	$2.16^{+0.77}_{-0.40}$	$5.57^{+0.57}_{-0.48}$	$4.50^{+0.66}_{-0.70}$
C-statistic (dof)	440(489)	477(489)	454(489)	480(489)	470(489)
Pearson χ^2 (dof)	498(489)	503(489)	497(489)	487(489)	483(489)
goodness	0.63	0.67	0.63	0.55	0.35
counts(10^3)	1.67	2.77	1.54	2.21	2.82
area (pixel^2)	61.32	69.63	76.50	80.19	80.63
Weighted by counts					
$kT_e\,(keV)$			$0.68^{+0.05}_{-0.05}$		
$n_e t, (10^{11}\,\mathrm{cm^{-3}\,s})$			$1.73^{+0.46}_{-0.46}$		

Supernova Remnant Evolution

Evolution of the SNR depends on the explosion energy, the ejected mass and the details of the surrounding medium. The position of the forward shock and reverse shock depends on the amount of material the forward shock has encountered.

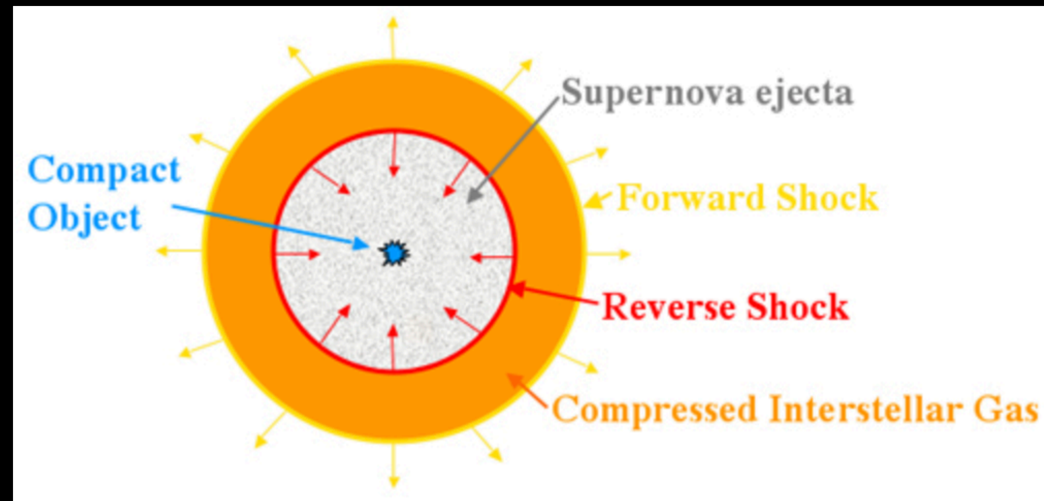

Truelove & McKee (1999)

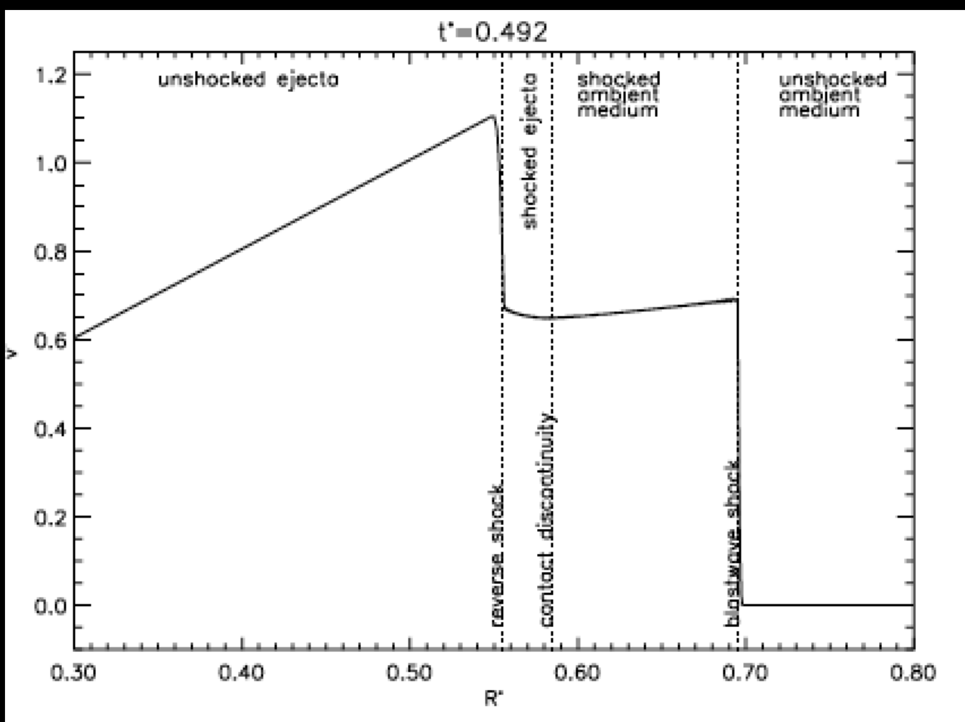

Micelotta et al. (2016) for s=2 case

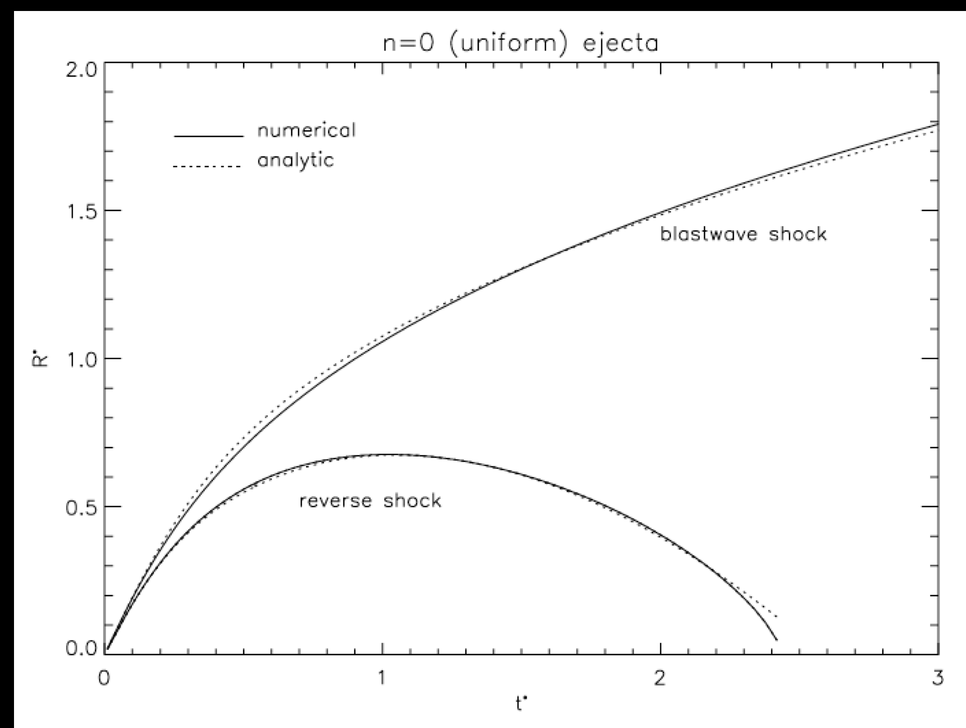

Evolutionary Models I

Xi et al. 2019

- we measure the blastwave velocity R_b, the reverse shock velocity R_r, and the blast wave velocity (v_b). *We know three things.*
- a grid of models were run for different ejecta masses (M_{ej}), circumstellar density profiles (s=0,2), & ejecta profile (n=9) based on Truelove & McKee (1999), Laming & Hwang (2003), and Micelotta et al. (2016). We search for the explosion energy (E_o) and circumstellar densities (ρ_0) that matches R_b, R_r, & v_b,
- we can reproduce R_b, R_r, & v_b, for ejecta masses between M_{ej}=2-6 but there is a large variation in the derived quantities, explosion energy (E_o), cirsumstellar density, etc.
- assuming the true explosion energy was in the range of 0.5-1.0 x10^{51} ergs, the s=2 prefers M_{ej}=3-6 but the swept-up mass values are large. The s=0 case prefers M_{ej}=2-3

Table 11. Models for ejecta profile $n = 9$, $R_b = 6.34$ pc, $R_r = 4.17$ pc and $v_b = 1614$km s^{-1}

Parameters	Symbol(units)	$s = 2$					$s = 0$				
Ejecta mass	$M_{ej}(M_\odot)$	2	3	4	5	6	2	3	4	5	6
Explosion energy	$E(10^{51}$ erg)	0.34	0.51	0.68	0.85	1.02	0.87	1.31	1.74	2.18	2.61
Circumsteller density	ρ_0(amu cm^{-3})	0.22	0.33	0.44	0.55	0.66	0.85	1.27	1.69	2.11	2.54
Swept-up mass	$M_\odot$	17.4	26.1	34.8	43.5	52.2	22.1	33.2	44.2	55.3	66.3
core mass	$M_\odot$	1.3	2.0	2.7	3.3	4.0	1.3	2.0	2.7	3.3	4.0
Unshocked mass	$M_\odot$	0.06	0.09	0.12	0.15	0.18	0.05	0.08	0.10	0.13	0.16

Evolutionary Models II

Xi et al. 2019

- the s=2 case gives an larger age than the Finkelstein estimate but still consistent at the 1 σ level. The s=0 age is consistent with previous estimates
- the s=0 indicates that E0102 has almost reached the Sedov phase and the reverse shock velocity in the observer frame is close to zero
- circumstellar densities of ~1.0 amu cm^{-3} imply unrealistically large mass loss rates, 10^{-4} $M_\odot$/yr for v_w=10 km/s and 10^{-2} $M_\odot$/yr for v_w=1000 km/s. But these 1D models assume isotropic and constant mass loss rates.

Table 12. The age, reverse shock velocity, upstream ejecta velocity, downstream ejecta velocity, and expansion parameter for the s=2 and s=0 cases.

Parameters	Symbol(units)	$s = 2$	$s = 0$
Age	yr	2642^{+1002}_{-489}	1730^{+552}_{-400}
Reverse shock velocity	$v_r(\mathrm{km s^{-1}})$	923^{+413}_{-314}	37^{+306}_{-185}
Upstream ejecta velocity	$v_{r,u}(\mathrm{km s^{-1}})$	1544^{+369}_{-402}	2359^{+621}_{-597}
Downstream ejecta velocity	$v_{r,d}(\mathrm{km s^{-1}})$	1078^{+387}_{-333}	618^{+384}_{-288}
Expansion parameter	m	$0.69^{+0.06}_{-0.01}$	$0.45^{+0.01}_{-0.01}$

Conclusions

- Chandra-alone analysis gives an expansion of 0.025 +/- 0.006 %/yr
- This corresponds to a forward shock velocity of v_b= 1614 +/- 367 km s^{-1}, optical expansion velocity is v_b= 1966 +/- 193 km s^{-1}
- Assuming partial electron-ion equilibration due to Coulomb collisions and cooling due to adiabatic expansion this v_b implies a post-shock electron temperature of 0.84 +/- 0.20 keV which is consistent with the estimate from the X-ray spectral fits of 0.68 +/- 0.05 keV
- There has been significant deceleration of the blastwave and the remnant is evolving from the free expansion phase to the Sedov phase
- 1D Evolutionary models can reproduce the observed values of the forward shock radius, the reverse shock radius, and the shock velocity
- 1D Evolutionary models can not distinguish between a constant density medium or a medium shaped by the stellar wind of the progenitor. However, we believe it is likely the progenitor was a massive star with a significant stellar wind.
- Implied mass loss rates are unrealistically high for the isotropic and constant mass loss case. Need more complicated scenarios such as a WR phase that interacts with the previously ejected material and creates a cavity.